



Preparation of polyethersulfone nanofiltration membrane by UV photo-grafting and separation for dye solutions

Zhe Wang, Baoli Shi*, Lina Jia

College of Science, Northeast Forestry University, Harbin, Heilongjiang 150040, China, email: shi_baoli_nefu@163.com (B. Shi)

Received 2 July 2017; Accepted 16 September 2017

ABSTRACT

A water-phase grafting method under UV photo-radiation was used to modify self-made polyethersulfone nanofiltration membranes. *N,N'*-Methylenebisacrylamide (BIS) was used as grafting monomer and Ce(IV) was used as initiator. At 3 mmol/L BIS concentration, 0.04 mol/L Ce(IV) concentration, and 7 min irradiation duration, the membrane could be grafted with a sufficient amount of monomer. Through the analysis of field emission scanning electron microscopy and attenuated total reflectance Fourier transform infrared, it was found that the grafting reaction mainly occurred at the surface of the PES membranes. Five dilute dye aqueous solutions, including methylene blue, acid fuchsin, methyl orange, rhodamine B, and acid chrome blue K, were used to test the separation performances of the modified membranes. The separation performances were compared with the performances of the nanofiltration membranes which were made by other researchers. An equation containing spectral color, charge, and relative cutoff molecular weight was built to calculate the theoretical rejection of the different modified membranes. Except for methylene blue, the changing trend of rejection vs. BIS concentration between the theoretical and experimental values was same. For rhodamine B, acid fuchsin, and acid chrome blue K, the theoretical rejection was similar to the experimental rejection.

Keywords: Dye; Nanofiltration; Zeta potential; PES; Wastewater

1. Introduction

Industrialization has caused environmental pollution to be a global problem. More than 100,000 commercially available textile dyes are present in the market, and approximately 700,000–1,000,000 tons of dyes are produced while 280,000 tons are discharged to the global environment annually via effluent generated from the textile industry [1]. Indiscriminate discharge of dye wastewater produces serious toxic effects on aquatic organisms [2]. Therefore, choosing an appropriate processing method to treat textile wastewater is significant. Conventional treatment methods include physical, chemical, biochemical, and hybrid processes [3]. Physical methods include adsorption, coagulation–flocculation, and membrane separation [4]. Adopting some adsorbents is commonly used for the removal of dyes and heavy metals. However, the

adsorbent method is sometimes restrictive due to its high cost and adsorbent regeneration capacity [5]. Coagulation–flocculation is also widely used for dye removal due to its low capital cost and simple operation [6]. However, this method is sometimes ineffective for some soluble dyes [7]. Meanwhile, membrane separation technology has emerged as a leading separation technology over the past decade [8]. It is a flexible and effective technology used for the treatment of dye wastewater [9]. The main membrane processes include reverse osmosis (RO), ultrafiltration (UF), and nanofiltration (NF). RO is the inverse process of osmosis. The RO membrane possesses high rejection rate and good mechanical stability [10,11]. However, RO is not suitable for application in dye wastewater treatment because of its weak pollution resistance [12]. For the UF membrane, the cutoff molecular weight is generally greater than the molecular weight of the dye molecule. Therefore, it is not suitable for the direct treatment of dye wastewater [13]. Meanwhile, NF membrane has become popular due to its low operation pressure and relatively low

* Corresponding author.

operation costs [14]. NF has become a potential technology for treating dye wastewater because the pore size of the separation layer is similar to the molecular size of dyes, although the deep reason of a nanofiltration membrane shows different rejection performances on dye molecules with similar molecular weight have not been put forward [15].

The current preparation methods of nanofiltration membrane mainly include phase inversion and combination. The phase inversion method is a very simple method. However, nanofiltration membrane with high separation performance cannot be prepared directly by this method. Combining the phase inversion method with other methods, such as surface modification, cross-linking, layer-by-layer self-assembly, and interfacial polymerization, researchers can easily adjust the pore structure to obtain a high-performance membrane. Among them, the surface modification has attracted considerable attention due to its simple operation, low cost, fast reaction, and no influence on the internal structure of membrane.

The surface modification methods mainly include physical and chemical modifications [16]. Physical modification methods consist of surface coating and material blending [17]. It is simple and easy to operate, but it could not achieve permanent modification. Chemical modification can be achieved by bulk modification and surface grafting. Grafting a functional monomer to the surface of polymer NF membrane is a beneficial technique because it can change the surface property without adverse influence on its bulk properties [18]. For the graft experiments, the commonly used monomers include acrylic acid, vinyl sulfonic acid, and *N,N'*-methylenebisacrylamide (BIS). Among them, BIS possesses two highly active double bonds that can easily combine to active points on the surface of the membrane. BIS also contains an amino group, which can improve the hydrophilicity of the modified membrane [19].

In this work, polyethersulfone (PES) composite membrane was first prepared through phase inversion. Then, BIS was grafted to the surface of the composite membrane by UV photo-grafting method to reduce the pore size to nanometer range. The performance of the grafted membrane was measured by separating five kinds of dyes. An empirical equation for calculating the rejection of the membrane was built, which included spectral color, charge, and relative cutoff molecular weight.

2. Material and methods

2.1. Materials

PES was purchased from BASF Co., Germany. Polyvinylpyrrolidone (PVP) K30 purchased from BASF, Germany, was utilized as pore former. Dimethylacetamide (DMAc) purchased from Tianjin Kermel Chemical Reagents Development Centre, China, was used as solvent. BIS was purchased from Maya Reagent Co., Ltd., China. Cerium sulfate ($\text{Ce}(\text{SO}_4)_2$) and iodine (I_2) were purchased from Tianjin Bodi Chemical Reagent Co., Ltd., China. Cerium chloride (CeCl_3) was purchased from Tianjin Kermel Chemical Reagents Development Centre, China. Sulphuric acid (H_2SO_4) was purchased from Beijing Chemical Reagents Development Centre, China. Barium chloride (BaCl_2) and polyethylene glycol-1000 (PEG-1000) were purchased from Tianjin Guangfu Chemical

Co., Ltd., China. Potassium iodide (KI) was purchased from Tianjin Ruijinte Chemicals Co., Ltd., China. Methylene blue, acid fuchsin, methyl orange, rhodamine B, and acid chrome blue K were purchased from Tianjin Guangfu Chemical Co., China. The structure and property of the five dyes are given in Table 1.

2.2. Preparation of PES membrane by phase inversion method

The immersion precipitation phase inversion method was used to prepare the membrane, as reported in our previous work [20]. PES powder was dried at 80°C for at least 24 h before using. A casting solution was prepared by blending PES, PVP, and DMAc. In the casting solution, the PES and PVP concentrations were 16 and 5 wt%. After complete dissolution and degassing, the solution was cast on a polyethylene terephthalate nonwoven fabric support by using a hand-casting knife with a 350 μm knife gap. Then the membrane was immersed in coagulation water. The prepared membrane was washed and stored in water for at least 1 day to completely leach out the residual solvent and additive before the next modification step by UV photo-grafting. The average rejection to PEG-1000 of the membrane was 78%.

2.3. Modification by UV photo-grafting

The PES membrane was modified by using a UV photo-grafting technique on a self-made device. Fig. 1 presents a schematic of the experimental device. A UV lamp (40 cm length, 500 W) was installed over the membrane. The distance between the lamp and the membrane was 20 cm. The lamp produced approximately 5.0 mW/cm^2 irradiation intensity on the membrane surface. The light intensity was measured with a UV irradiance meter (model XYI-V, Hangzhou Xinye Optoelectronic Engineering Co., Ltd., China).

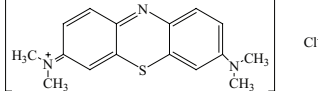
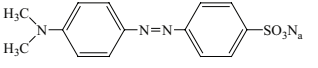
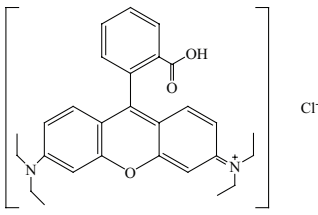
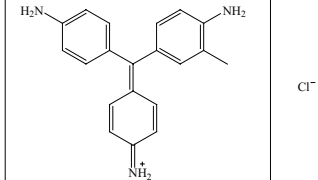
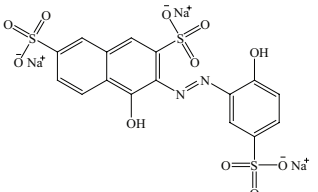
The UV photo-grafting modification was performed in three steps. In the first step, grafting aqueous solution was prepared including BIS, the initiator ($\text{Ce}(\text{SO}_4)_2$ and CeCl_3), and 5% H_2SO_4 . The monomer concentrations were 1, 3, and 6 mmol/L and the quantity of the initiator was 50 mg. In the second step, the grafting solution was sprayed onto the membrane. The pristine membrane with a size of 30 cm \times 30 cm was placed on the self-made device and the grafting solution was sprayed at the surface of the pristine membrane at room temperature. The third step was sending the sprayed membrane into the trunk, with the membrane receiving UV-irradiation for 7 min to complete the grafting reaction. During the UV irradiation, the evaporation of water did not cause the decrease of the content of the monomer.

Fig. 2 presents the two-step reaction mechanism of grafting BIS to PES chains. In the first step, PES chains at the surface of the polymer membrane were oxidized by Ce^{4+} to produce sulfur radicals. In the second step, vinyl groups of BIS then react with the sulfur radicals, forming grafted groups [21].

2.4. Characterization of membranes

Field emission scanning electron microscopy (FESEM, FEI Sirion, Netherlands) was employed for morphology characterization of the membranes. Membranes were cut into small pieces and cleaned with filter paper. The pieces were

Table 1
Structure and property of dye

Name	Structure	Molecular weight	Maximum absorption wavelength (nm)
Methylene blue		319.85	664
Methyl orange		327.33	463
Rhodamine B		479.02	556
Acid fuchsin		585.53	545
Acid chrome blue K		586.40	522

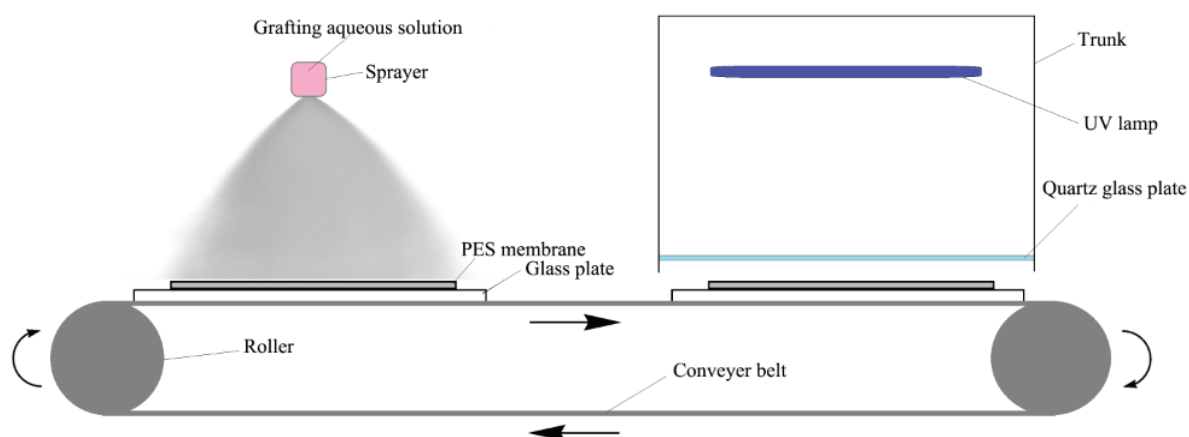


Fig. 1. Schematic of UV photo-grafting experimental device.

broken and kept in air for drying. The dried samples were gold sputtered for FESEM observation.

The contact angle of membranes was measured by a contact angle measuring instrument (DSA100S). The measurements were performed at room temperature. A total of 5.0 μL pure water was dropped at the top surface of the

sample. Each sample was measured three times at different locations of the membrane to evaluate the average value. All the membranes were fully dried before measuring.

The chemical groups at the top surface of the membranes were analyzed using an attenuated total reflectance Fourier transform infrared (AT-FTIR) spectroscopy technique

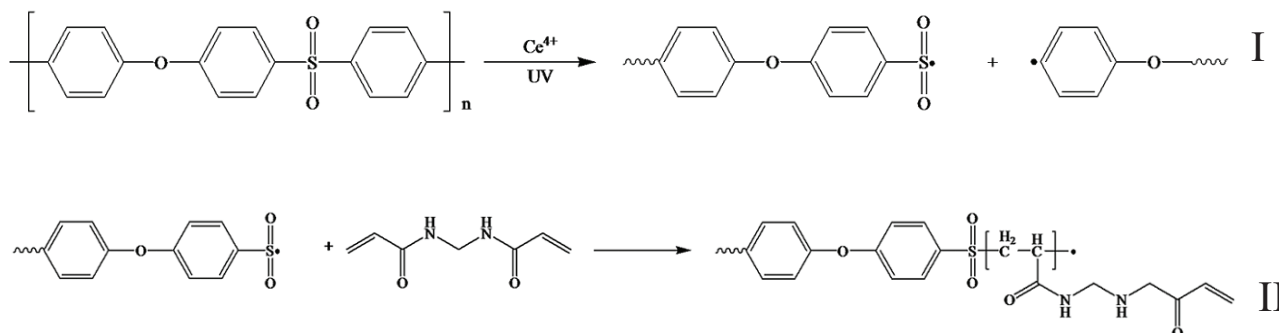


Fig. 2. Reaction mechanism of grafting BIS to PES chains.

performed with a Nicolet FTIR 360 spectrometer. The surface of the membranes was in contact with a ZnSe crystal with a 45° incidence angle. Absorption spectra were taken at 4 cm⁻¹ resolution between 4,000 and 650 cm⁻¹.

The zeta potential (ζ) was measured to quantify the charge of the surface of PES membrane. It was measured based on KCl solutions with concentrations of 1, 2, 3, 4, and 5 mmol/L. The KCl solutions with different concentrations were flowed on the surface of PES membranes with a size of 10 cm × 0.5 cm. The zeta potential was measured according to the Helmholtz-Smoluchowski equation [22] (given in Eq. (1)).

$$\zeta = K_0 \frac{\kappa \times \eta \times E}{\varepsilon \times \Delta P} \quad (1)$$

where K_0 is the correction factor of equipment, κ is the conductivity of solution, η is the solution viscosity, E is the streaming potential, ε is the dielectric constant, ΔP is the pressure difference (given in Table S1). In the equation, the viscosity (η) and dielectric constant (ε) of the solutions were measured by a viscometer and a dielectric constant meter, respectively. The conductivity (κ) of the solutions was measured by a conductivity meter.

The permeability of the membranes for concentrating five dilute dye aqueous solutions was measured at room temperature and was expressed by flux and rejection. The experiment was performed with a self-made filtration equipment and cross-flow operation was adopted. The area of the membranes was 13 cm² and the concentration of dye solutions was 10–30 mmol/L. Initially, the membranes were pre-pressurized in pure water for 20 min at 0.3 MPa before the measurement. Then, the water was replaced by the dye solutions. After the permeation state stabilized, the pressure was changed to 0.2 MPa. Then, the liquid volume and the changes of the concentration were recorded. For each dye solution and membrane, data were measured for at least three times. The water flux, J (L/(m²·h)), was calculated by Eq. (2).

$$J = \frac{V}{S \Delta T} \quad (2)$$

where V (L) is the quantity of the permeate, S (m²) is the membrane area, and ΔT (h) is the permeation time. Rejection (%) was calculated with Eq. (3).

$$R = \left(1 - \frac{C_p}{C_f} \right) \times 100 \quad (3)$$

where C_p and C_f are the concentrations of the permeation and feed, respectively. The concentration was measured with an UV-Vis spectrophotometer (T6, Beijing Purkinje General Instrument, China) at the maximum absorption wavelength of each dye.

3. Results and discussion

Figs. 3 and 4 show the cross-section FESEM morphologies of the unmodified and modified membranes prepared at a BIS concentration of 3 mmol/L, respectively. No obvious change was observed in the cross-section morphology of the modified membrane after the grafting treatment.

Fig. 5 shows the top surface FESEM morphologies of the unmodified and modified membranes prepared at the BIS concentration of 3 mmol/L, respectively. It shows that the top surface of the modified membrane is smoother than that of the unmodified membrane. The average rejection to PEG-1000 of the modified membrane was 80%.

The water contact angle value of the unmodified PES membranes and modified PES membranes was 54.8° and 32.8°, respectively. This result can be attributed to the introduction of amine group to the modified membrane because the amine group is a hydrophilic group.

Fig. 6 presents the AT-FTIR spectra of the unmodified membrane and the modified membrane prepared under the same conditions as described above. The absorption peaks at 3,064 and 2,965 cm⁻¹ are attributed to C–H stretching vibration of benzene ring of PES chain. The absorption peak at 1,660 cm⁻¹ is the C=O stretching vibration of the amide group of BIS. The C–H groups in PES chains are replaced by C=O groups in BIS chains. Therefore, as shown in the FESEM photographs, the AT-FTIR spectra prove that BIS was successfully grafted to the surface of PES membrane.

Fig. 7 shows the plot of the zeta potential vs. the monomer concentration for the modified membranes. It shows that the zeta potential initially decreases and then increases with the increase of the monomer concentration. With the increase of monomer concentration, the surface charge density of the PES membranes initially increases and then decreases. The charge density reached the maximum when the concentration of BIS was 1 mmol/L. The reasons are as follows: with the first step of the reaction, a large number of sulfur free radicals were produced. At this time, the concentration of BIS was low and could not fully react. Therefore, the surface of the membrane contained a large amount of charge. The zeta potential was at

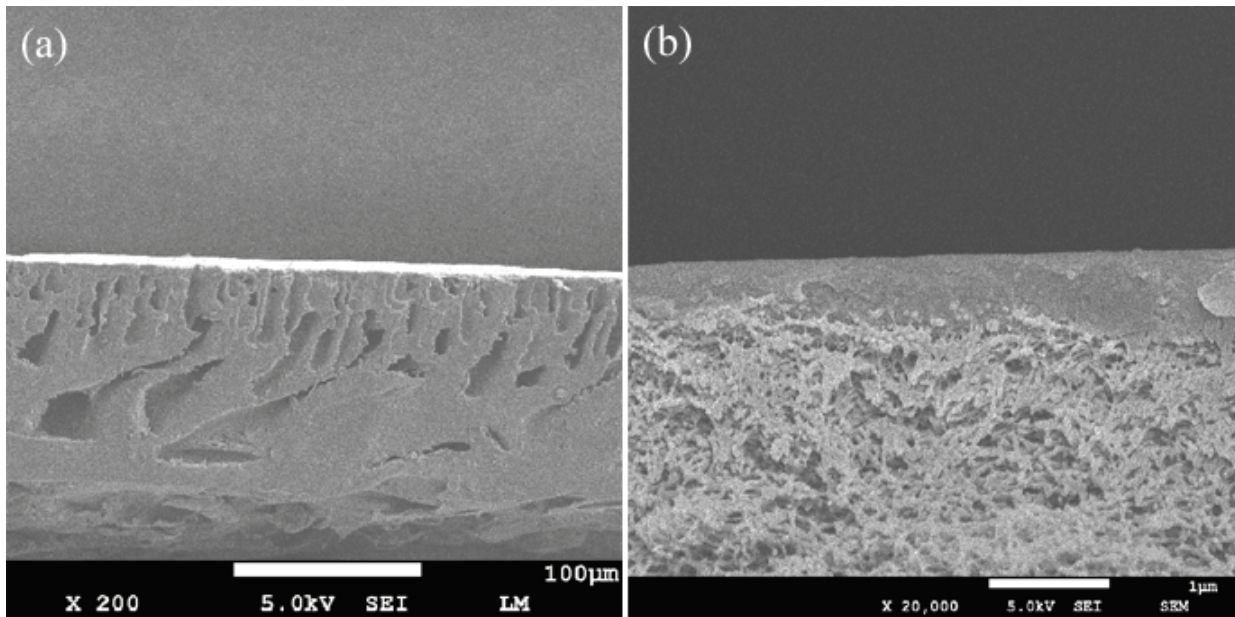


Fig. 3. Cross-section FESEM morphologies of unmodified PES membranes: (a) magnification of 200 \times and (b) magnification of 20,000 \times .

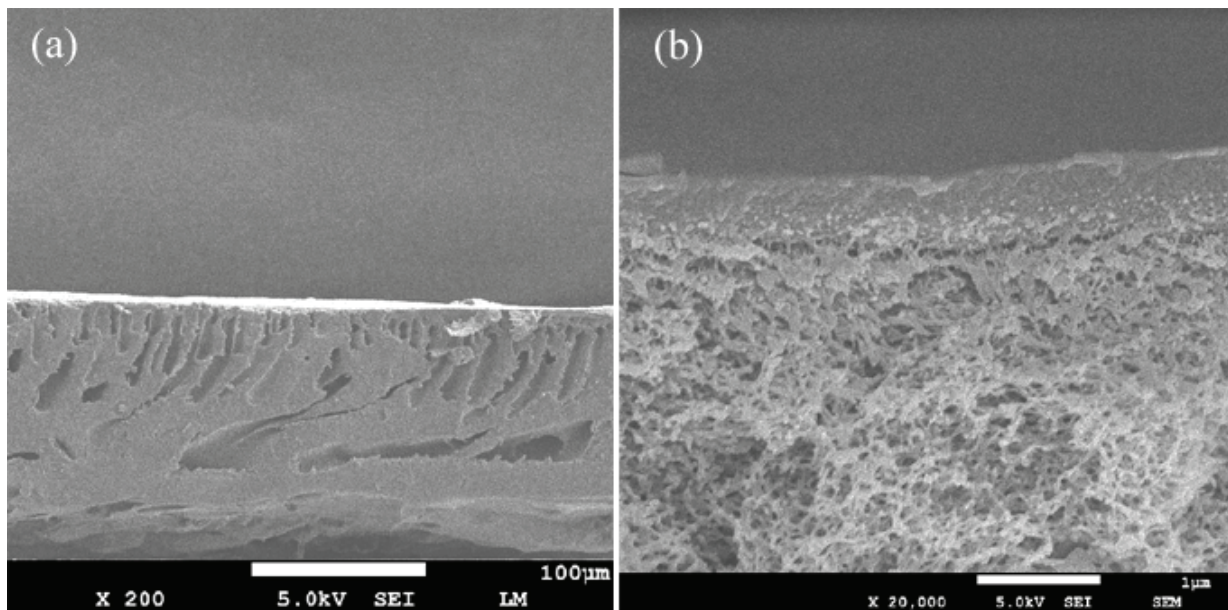


Fig. 4. Cross-section FESEM morphologies of modified PES membranes prepared at BIS concentration of 3 mmol/L: (a) magnification of 200 \times and (b) magnification of 20,000 \times .

its maximum. Then, with the increase of the concentration of BIS and the increase of reaction extent, the content of sulfur radical decreases and the zeta potential decreases.

Fig. 8 shows the plot of flux vs. the monomer concentration for the modified membranes. It shows that the flux of all the dye solutions decreases with the increase of the monomer concentration. The reason for this phenomenon may be: the PES membrane was gradually compressed during operation, and the dye molecules were adsorbed on the surface of the membrane and even the pore of the membrane. The pore size of the membrane decreased. The permeability resistance increased and the flux decreased.

Fig. 9 shows the variation tendency of the rejection of the modified membranes with the monomer concentration. With the increase of the monomer concentration, the rejection for all the dyes increases. The separation performance of the nanofiltration membrane was compared with other membranes as listed in Table 2. For dyes with similar molecular weights, the rejection of the modified PES membrane was higher than that of the others.

In Fig. 9, for different dyes, the changing trend of rejection with BIS concentration is different. According to the analysis of Esmaili et al., the factors affecting the rejection include charge and pore size, etc. [26]. Because the color of a matter is also

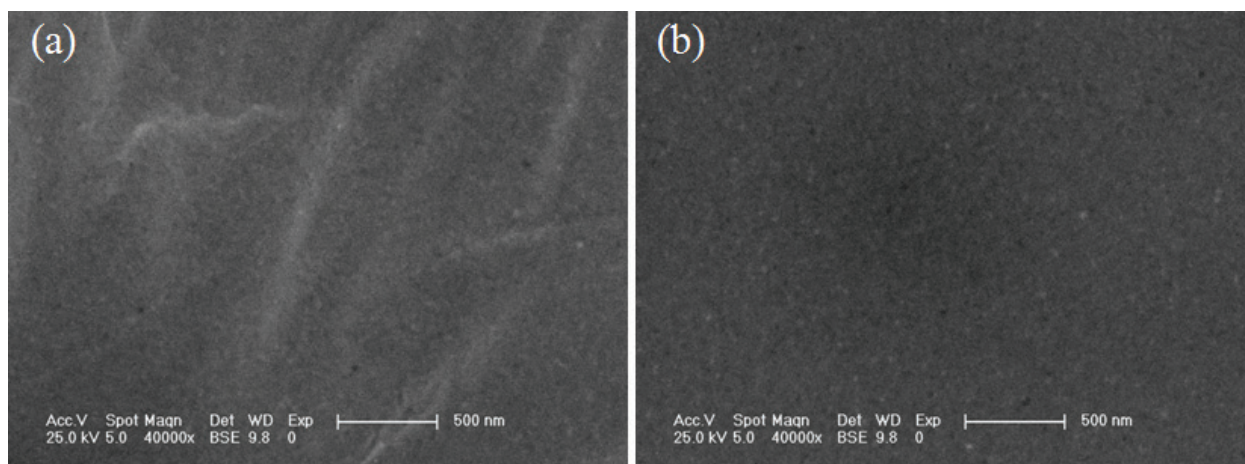


Fig. 5. Surface FESEM morphologies of (a) the unmodified PES membranes and (b) the modified PES membranes prepared at BIS concentration of 3 mmol/L.

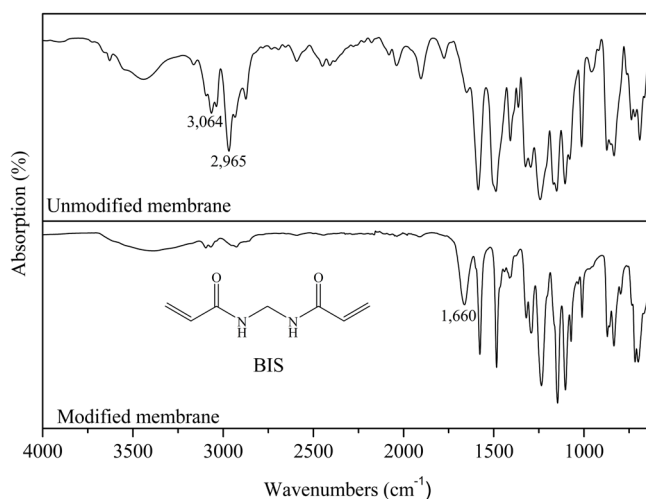


Fig. 6. AT-FTIR spectra of the unmodified membrane and modified membrane prepared at BIS concentration of 3 mmol/L.

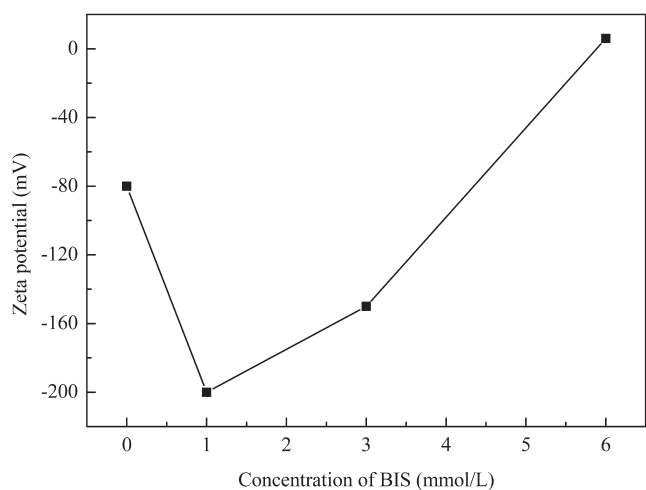


Fig. 7. Plot of zeta potential vs. monomer concentration for the modified membranes.

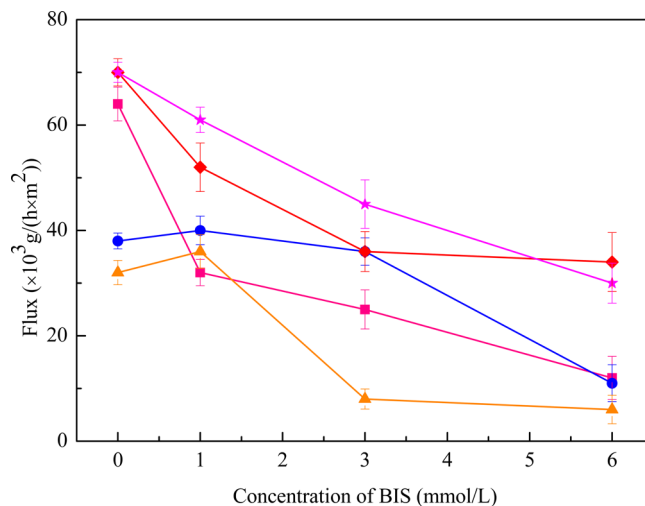


Fig. 8. Plot of flux vs. monomer concentration for the modified membranes. ★: Rhodamine B, ◆: acid fuchsin, ▲: methyl orange, ■: acid chrome blue K, and ●: methylene blue.

decided by its intermolecular force, we thought that the rejection may be was also related with the color parameter when the molecular weight of different dyes was similar. Then, we built an equation containing spectral color, charge, and relative cut-off molecular weight to calculate the theoretical rejection and compared it with the experimental rejection as follows.

$$R = C_1 \times (F_d \times F_m) + C_2 \times (C_d \times C_m) + C_3 \times (A_d \times \gamma - A_m) \quad (4)$$

where C_1 , C_2 , and C_3 are the coefficient of spectral color, charge coefficient, and coefficient of relative cutoff molecular weight, respectively. The values of C_1 , C_2 and C_3 are 2.3, 0.12, and 0.12, respectively. F_d and F_m are the visible wavelength of the dye and membranes, respectively. C_d and C_m are the molecular charge of dye and charge of membranes, which was considered as the zeta potential. A_d and A_m are the molecular size of dye and relative pore size of membrane. γ is the symmetric coefficient of dye molecule as given in Table S2.

Table 3 lists the parameters of the dye molecules and the nanofiltration membranes which were determined according to the visible wavelength, the molecular weight, and the quantity of electric charge.

According to Eq. (4) and the values listed in Table 3, the theoretical rejection of dyes was calculated at different

monomer concentrations. Fig. 10 shows the experimental rejection and the theoretical rejection vs. the concentration of BIS. Except for methylene blue, the theoretical rejection was similar to the experimental rejection. Especially for methyl orange, the data were almost completely similar. For the others, the experimental values possessed the same trend

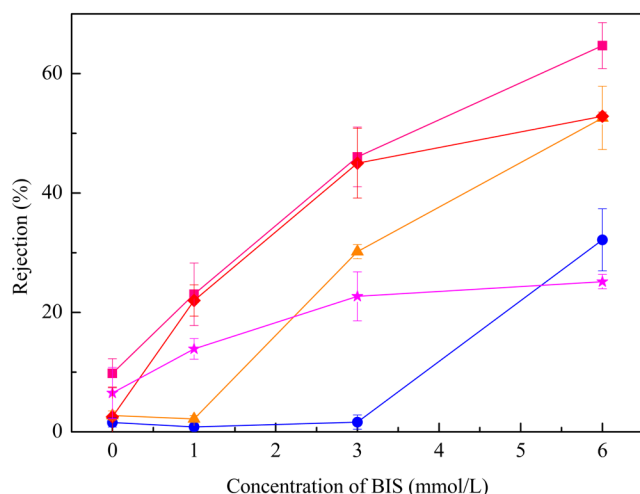


Fig. 9. Plot of rejection vs. BIS concentration. \star : Rhodamine B, \diamond : acid fuchsin, \triangle : methyl orange, \blacksquare : acid chrome blue K, and \bullet : methylene blue.

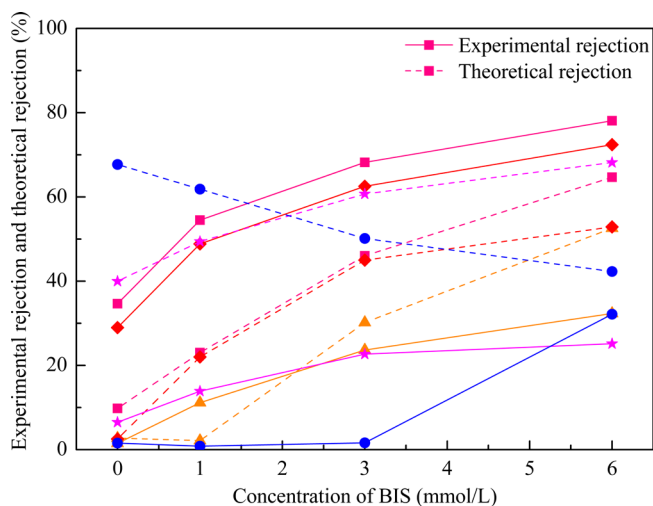


Fig. 10. Plot of experimental rejection and theoretical rejection vs. concentration of BIS, \star : Rhodamine B, \diamond : acid fuchsin, \triangle : methyl orange, \blacksquare : acid chrome blue K, and \bullet : methylene blue.

Table 2
Rejection of membrane to dyes

Membrane name	Dye name	Molecular weight	Rejection (%)
Self-made modified PES membrane (BIS concentration 6 mmol/L)	Methyl orange	327	63
	Acid fuchsin	585	50
	Acid chrome blue K	586	51
PEC membranes [23]	Methyl orange	327	6
	Acid fuchsin	585	82
	Rose bengal	558	98
PEI membrane [24]	Safranin O	350	99
	Orange II	350	59
sPPSU membrane [25]	Reactive blue 19	627	82
	Reactive black 5	992	84
	Reactive yellow 81	1,630	86

Table 3
Influence factor of rejection

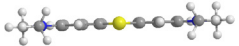
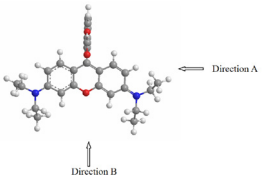
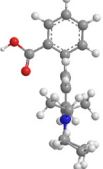
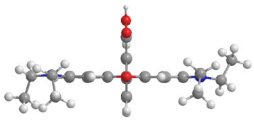
Dye name	F_d	C_d	A_d	Membrane name	F_m	C_m	A_m
Methylene blue	440	1	284	Pure membrane	630	0	540
Methyl orange	630	-1	304	Modified membrane 1 ^a	610	-130	320
Rhodamine B	700	1	443	Modified membrane 2 ^b	580	-160	300
Acid fuchsin	700	-3	539	Modified membrane 3 ^c	560	-190	280
Acid chrome blue K	700	-3	517				

^aMonomer concentration: 1 mmol/L.

^bMonomer concentration: 3 mmol/L.

^cMonomer concentration: 6 mmol/L.

Table 4
The three-dimensional model and the minimum area of methylene blue and rhodamine B

Name	Vertical view	Direction A	Direction B	Minimum area (\AA^2)
Methylene blue				10.85
Rhodamine B				37.90

as the theoretical values, although the data were slightly different. The main reasons of the deviations may be as follows: first, in the calculation of the theoretical rejection, the symmetry coefficient was given while the three-dimensional molecules were regarded as planar molecules and the steric properties of molecules were ignored. Second, in the process of estimating the relative cutoff molecular weight, there may be few differences between the experimental value and the theoretical value. Estimating the experimental rejection with the theoretical rejection is feasible, although some deviations were observed between them.

For methylene blue, the trend between the experimental and theoretical rejection was the opposite. The possible reason for this phenomenon is as follows: by simulating the spatial structure of the dye molecules with software, we found that methylene blue was more inclined to a planar shape, while the other dyes had stronger stereoscopic shape and tended to be spherical as listed in Table 4. Therefore, the interaction between methylene blue and the membrane pores was different from that of the other dye molecules. Given that the molecular weight of methylene blue was the lowest, the effect of spatial shape would be a decisive factor compared with the charge and color factors.

4. Conclusion

When Ce(IV) was used as the initiator and BIS as the monomer, BIS could be grafted to the surface of pure PES membrane through the water-phase grafting method under UV photo-radiation. For five dye solutions, the rejection of the modified nanofiltration membrane reached the highest values when the grafting conditions were: BIS concentration was 6 mmol/L, Ce(IV) concentration was 0.04 mol/L, and irradiation duration was 7 min. An equation containing spectral color, charge, and relative cutoff molecular weight was built to calculate the theoretical rejection of the different modified membranes. Except for methylene blue, the changing trend of rejection vs. BIS concentration between the theoretical and experimental values was same. For rhodamine B, acid fuchsin, and acid chrome blue K, the theoretical rejection was similar to the experimental rejection.

Acknowledgment

The authors acknowledge the financial support by Harbin Applied Technology Research and Development Project (2016RAQXJ011).

References

- [1] V. Jegatheesan, B.K. Pramanik, J. Chen, D. Navaratna, C.Y. Chang, C. Shu, Treatment of textile wastewater with membrane bioreactor: a critical review, *Bioresour. Technol.*, 204 (2016) 202–212.
- [2] B. Bethi, S.H. Sonawane, B.A. Bhanvase, S.P. Gumfekar, Nanomaterials based advanced oxidation processes for waste water treatment: a review, *Chem. Eng. Process. Process Intensif.*, 109 (2016) 178–189.
- [3] C.Z. Liang, S.P. Sun, F.Y. Li, Y.K. Ong, T.S. Chung, Treatment of highly concentrated wastewater containing multiple synthetic dyes by a combined process of coagulation/flocculation and nanofiltration, *J. Membr. Sci.*, 469 (2014) 306–315.
- [4] A.Y. Zahrim, N. Hilal, Treatment of highly concentrated dye solution by coagulation/flocculation–sand filtration and nanofiltration, *Water Resour. Ind.*, 3 (2013) 23–34.
- [5] S.D. Gisi, G. Lofrano, M. Grassi, M. Notarnicola, Characteristics and adsorption capacities of low-cost sorbents for wastewater treatment: a review, *Sustain. Mater. Technol.*, 9 (2016) 10–40.
- [6] E. Gilpavas, I. Dobrosz-Gómez, M.Á. Gómez-García, Coagulation-flocculation sequential with Fenton or photo-Fenton processes as an alternative for the industrial textile wastewater treatment, *J. Environ. Manage.*, 191 (2017) 189.
- [7] T. Chen, B. Gao, Q. Yue, Effect of dosing method and pH on color removal performance and floc aggregation of polyferric chloride–polyamine dual-coagulant in synthetic dyeing wastewater treatment, *Colloids Surf., A*, 355 (2010) 121–129.
- [8] Y. Magara, S. Kunikane, M. Itoh, Advanced membrane technology for application to water treatment, *Water Sci. Technol.*, 37 (1998) 91–99.
- [9] X. Zheng, Z. Zhang, D. Yu, X. Chen, R. Cheng, S. Min, J. Wang, Q. Xiao, J. Wang, Overview of membrane technology applications for industrial wastewater treatment in China to increase water supply, *Resour. Conserv. Recycl.*, 105 (2015) 1–10.
- [10] S. Bou-Hamad, M. Abdel-Jawad, M. Al-Tabtabaei, S. Al-Shammari, Comparative performance analysis of two seawater reverse osmosis plants: twin hollow fine fiber and spiral wound membranes, *Desalination*, 120 (1998) 95–106.
- [11] H.A. Shawky, Performance of aromatic polyamide RO membranes synthesized by interfacial polycondensation process in a water–tetrahydrofuran system, *J. Membr. Sci.*, 339 (2009) 209–214.

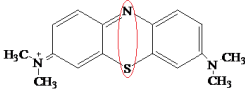
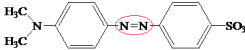
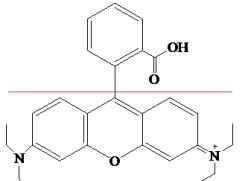
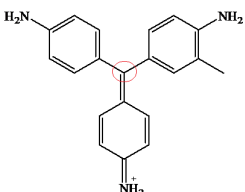
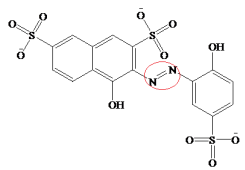
- [12] C. Li, C. Song, P. Tao, M. Sun, Z. Pan, T. Wang, M. Shao, Enhanced separation performance of coal-based carbon membranes coupled with an electric field for oily wastewater treatment, *Sep. Purif. Technol.*, 168 (2016) 47–56.
- [13] T. Bilstad, E. Espedal, Membrane separation of produced water, *Water Sci. Technol.*, 34 (1996) 239–246.
- [14] S. Cheng, D.L. Oatley, P.M. Williams, C.J. Wright, Positively charged nanofiltration membranes: review of current fabrication methods and introduction of a novel approach, *Adv. Colloid Interface Sci.*, 164 (2011) 12–20.
- [15] A.K. An, J. Guo, S. Jeong, E.J. Lee, S.A.A. Tabatabai, T. Leiknes, High flux and antifouling properties of negatively charged membrane for dyeing wastewater treatment by membrane distillation, *Water Res.*, 103 (2016) 362–371.
- [16] F. Li, J. Ye, L. Yang, C. Deng, Q. Tian, B. Yang, Surface modification of ultrafiltration membranes by grafting glycine-functionalized PVA based on polydopamine coatings, *Appl. Surf. Sci.*, 345 (2015) 301–309.
- [17] M. Amirilargani, M. Sadrzadeh, E.J.R. Sudhölter, L.C.P.M. Smet, Surface modification methods of organic solvent nanofiltration membranes, *Chem. Eng. J.*, 289 (2015) 562–582.
- [18] A. Rahimpour, UV photo-grafting of hydrophilic monomers onto the surface of nano-porous PES membranes for improving surface properties, *Desalination*, 265 (2011) 93–101.
- [19] F.Y. Li, Production and application of methylene-bisacrylamide, *Fine Chem. Ind. Raw Mater. Intermed.*, 5 (2006) 29–31.
- [20] Q.R. Zhang, The Study of Preparation of Polyethersulfone/Polyimide Alloy Nanofiltration Membrane, China National Knowledge Infrastructure, 2009.
- [21] A.W. Mohammad, Y.H. Teow, W.L. Ang, Y.T. Chung, D.L. Oatley-Radcliffe, N. Hilal, Nanofiltration membranes review: recent advances and future prospects, *Desalination*, 356 (2015) 226–254.
- [22] P. Mou, S.D. Jons, Chemistry and fabrication of polymeric nanofiltration membranes: a review, *Polymer*, 103 (2016) 417–456.
- [23] M. Bastin, K. Hendrix, I. Vankelecom, Solvent resistant nanofiltration for acetonitrile based feeds: a membrane screening, *J. Membr. Sci.*, 536 (2017) 176–185.
- [24] P.S. Zhong, N. Widjojo, T.S. Chung, M. Weber, C. Maletzko, Positively charged nanofiltration membranes via UV grafting on sulfonated polyphenylenesulfone for effective removal of textile dyes from wastewater, *J. Membr. Sci.*, 417–418 (2012) 52–60.
- [25] Y.K. Ong, F.Y. Li, S.P. Sun, B.W. Zhao, C.Z. Liang, T.S. Chung, Nanofiltration hollow fiber membranes for textile wastewater treatment: lab-scale and pilot-scale studies, *Chem. Eng. Sci.*, 114 (2014) 51–57.
- [26] S. Esmaeili, M. Rahbar, H. Pahlavanzadeh, S. Ayatollahi, Investigation of streaming potential coupling coefficients and zeta potential at low and high salinity conditions: experimental and modeling approaches, *J. Petrol. Sci., Eng.*, 145 (2016) 137–147.

Supplementary material

Table S1
Data of Helmholtz-Smoluchowski equation

Name	KCl concentration (mmol/L)	Monomer concentration (mmol/L)	ΔP (Pa)	ϵ (F/m)	η (cP)	E (V)	κ ($\Omega\cdot\text{m}$)	ζ (mV)
PES membrane	1	0	2,533	24.96	0.89	13.1	0.28	54.67
PES membrane	2	0	2,533	24.95	0.89	5.0	0.16	107.85
PES membrane	3	0	2,533	24.99	0.89	4.0	0.11	66.29
Pure membrane	4	0	2,533	24.84	0.89	2.7	0.08	70.17
PES membrane	5	0	2,533	25.01	0.89	3.5	0.07	78.52
PES membrane	1	1	2,533	24.96	0.89	6.57	0.28	25.04
PES membrane	2	1	2,533	24.95	0.89	-2.0	0.16	112.17
PES membrane	3	1	2,533	24.99	0.89	-2.7	0.11	210.46
PES membrane	4	1	2,533	24.84	0.89	-2.3	0.08	415.82
PES membrane	5	1	2,533	25.01	0.89	-6.5	0.07	383.63
PES membrane	1	3	2,533	24.96	0.89	-3.5	0.28	49.93
PES membrane	2	3	2,533	24.95	0.89	9.6	0.16	-280.42
PES membrane	3	3	2,533	24.99	0.89	12.3	0.11	-311.80
PES membrane	4	3	2,533	24.84	0.89	12.0	0.08	-488.14
PES membrane	5	3	2,533	25.01	0.89	13.1	0.07	-206.57
PES membrane	1	6	2,533	24.96	0.89	15.0	0.28	-93.72
PES membrane	2	6	2,533	24.95	0.89	14.2	0.16	58.42
PES membrane	3	6	2,533	24.99	0.89	14.8	0.11	68.44
PES membrane	4	6	2,533	24.84	0.89	15.8	0.08	93.56
PES membrane	5	6	2,533	25.01	0.89	15.3	0.07	102.50

Table S2
Structure and symmetry of dye

Name	Structure and geometrical center	Molecular weight of A ^a (M _A)	Molecular weight of B ^a (M _B)	Symmetry coefficient (γ) ^b
Methylene blue cation		119.18	119.18	1
Methyl orange anion		120.19	152.12	1.2
Rhodamine B cation		121.12	322.49	2.7
Acid fuchsin cation		92.13	106.16	1.2
Acid chrome blue K anion		302.27	172.16	1.8

^aAccording to the symmetry center position, the left structure is defined as A, and the right side is defined as B.

^bSymmetry coefficient: $\gamma = M_A/M_B$.